On the Mechanism of Gas-Phase Reaction of C1−C3 Aliphatic Thiols + OH Radicals

Armando Cruz-Torres and Annia Galano*

Instituto Mexicano del Petróleo, Eje Central Lázaro Cárdenas 152, 07730, México D. F., México

Received: November 7, 2006; In Final Form: December 21, 2006

A theoretical study on the mechanism of the OH + aliphatic thiols reactions is presented. Optimum geometries and frequencies have been computed at the BHandHLYP/6-311++G(2d,2p) level of theory for all stationary points. Energy values have been improved by single-point calculations at the above geometries using CCSD(T)/6-311++G(d,p). Twelve possible channels have been modeled, three of them including the possible influence of molecular oxygen, and three of them involving excess of OH. The only channels that have been found to significantly contribute to the overall reaction in the troposphere are the hydrogen abstractions from the −SH group and from the alkyl groups. Our analysis supports a stepwise mechanism involving the formation of a short-lived, weakly bonded adduct in the entrance channel, for the abstraction paths. The results proposed in the present work seem to provide a viable explanation for diverse findings previously reported from experimental investigations.

Introduction

Reactions of hydroxyl radicals in the gas phase are central to atmospheric chemistry since the main sink of many volatile organic compounds (VOCs) involves reactions with them. Thiols are no exceptions; the atmospheric daytime oxidation process of thiols is initiated by reactions with the OH radical. Reduced organic sulfur compounds are mainly emitted from the sea surface and by biological activity. A number of these compounds have been detected in the atmosphere, including CH_3SH.[1] In addition, a large number of other organic sulfur compounds are known to be produced by microorganisms, including C_2H_5SH and n-C_3H_7SH.[2]

Several studies on the mechanism and reaction products of the aliphatic thiols + OH radical reactions have been carried out. Lee and Tang,[3] Wine et al.,[4] and Barnes et al.[5] found that all the thiols react with similar rate coefficients. Accordingly, they suggest that the reactions occur mainly by H abstraction from the SH group. Lee and Tang also reported that higher initial OH concentrations result in larger rate constants. In addition, Wine et al. also studied the CH_3SD + OH reaction and found its rate coefficient identical to that of CH_3SH. On the basis of their finding, they concluded that the dominant pathway is the addition to the sulfur atom. Hynes and Wine[6] found the reaction of CD_3SH to be 13% slower than that of CH_3SH, which proves that abstractions from the alkyl group also contribute to the overall reaction. These authors also found that the rate constants of the reactions of CH_3SH and CD_3SH with OH are independent of O_2 concentration. Hatakeyama and Akimoto[7] carried out end product analysis and suggested an addition pathway leading to $CH_3S(OH)H$ formation. On the other hand, Tyndall and Ravishankara[8] monitored the CH_3S radical via laser-induced fluorescence and showed that its production in the CH_3SH + OH reaction has a yield of unity. According to their results, the adduct must be short-lived. More recently, Butkovskaya and Setser[9] studied the same reaction and found that the abstraction of H atom from the methyl group accounts for (11 ± 4)% of the total reaction rate from the OD + CH_3SD (or OD + CH_3-SH) reaction and for (24 ± 8)% from the OH + CH_3SH (or OH + CH_3SD) reaction. Accordingly, the major product channel involves interaction with the sulfur end of the molecule. For the reactions at the sulfur end of the molecule, they also predict branching fractions of 0.24 for abstraction and 0.76 for addition−elimination. In summary, the mechanism for the reaction of OH with aliphatic thiols is still unclear.

The aim of this work is to model every feasible step of the reactions of OH with R−SH (R = CH_3, C_2H_5, and n-C_3H_7) and to provide further insight into their mechanism, which could hopefully lead to a viable explanation for the fact that these thiols react with OH at very similar rates. In addition, the present study could also provide useful information about the proportion in which the different products are formed.

Computational Details

Full geometry optimizations were performed with the Gaussian 98[10] program using the BHandHLYP hybrid HF-density functional and the 6-311++G(2d,2p) basis set. The energies of all the stationary points were improved by single-point calculations at the CCSD(T)/6-311++G(d,p) level of theory. Unrestricted calculations were used for open shell systems. Frequency calculations were carried out for all the stationary points at the DFT level of theory, and local minima and transition states were identified by the number of imaginary frequencies (NIMAG = 0 or 1, respectively). Intrinsic reaction coordinate (IRC) calculations were carried out at the BHandHLYP/6-311G++(d,p) level of theory to confirm that the transition state structures connect the proper reactants and products. Zero-point energies (ZPE) and thermal corrections to the energy at 298.15 K were included in the determination of the activation energies and of the heats of reaction, respectively.

The conventional transition state theory (TST)[11,12] was used to calculate the rate coefficients. The tunneling correction defined as the Boltzmann average of the ratio of the quantum and the classical probabilities was calculated using the Eckart method.[13] This method approximates the potential by a one-dimensional function that is fitted to reproduce the ZPE-corrected barrier, the enthalpy of reaction at 0 K, and the

* Corresponding author. E-mail: agalano@imp.mx.

10.1021/jp0673415 CCC: $37.00
Published on Web 02/06/2007

curvature of the potential curve at the transition state. This method tends to overestimate the tunneling contribution, especially at very low temperature, because the fitted Eckart function is often too narrow. However, sometimes it compensates for the corner-cutting effect not included in the Eckart approach.[14−16] Such compensation can lead to Eckart transmission coefficients similar[15] or even lower[16] than those obtained by the small-curvature tunneling method[17] at temperatures equal to or higher than 300 K. In addition, in this work, the partition function values have been corrected by replacing some of the large amplitude vibrations by the corresponding hindered internal rotations, when necessary.

The methodology used in the present work has been successfully used to quantitatively describe the kinetics and mechanism of gas-phase hydrogen abstraction reactions from diverse VOCs.[18−24]

Results and Discussion

Geometries and Energies. We have modeled 12 possible reaction paths for the smallest of the studied thiols to determine which ones are most likely to occur and, based on that previous knowledge, to model only those paths that are relevant to the overall reactions for the larger ones. The modeled paths for methyl thiol are:

$$CH_3SH + OH \rightarrow CH_3S(OH)H \rightarrow CH_3S + H_2O \quad (1)$$

$$CH_3SH + OH \rightarrow CH_3S(OH)H \rightarrow CH_2SH + H_2O \quad (2)$$

$$CH_3SH + OH \rightarrow CH_3S(OH)H \quad (3)$$

$$CH_3SH + OH \rightarrow CH_3S(OH)H \rightarrow CH_3S(O)H + H \quad (4)$$

$$CH_3SH + OH \rightarrow CH_3S(OH)H \rightarrow CH_3SOH + H \quad (5)$$

$$CH_3SH + OH \rightarrow CH_3S(OH)H \rightarrow HOSH + CH_3 \quad (6)$$

$$CH_3SH + OH + O_2 \rightarrow CH_3S(OH,O_2)H \quad (7)$$

$$CH_3SH + OH \rightarrow CH_3S(OH)H \xrightarrow{O_2} CH_3SOH + HO_2 \quad (8)$$

$$CH_3SH + OH \rightarrow CH_3S(OH)H \xrightarrow{O_2} CH_3S(O)H + HO_2 \quad (9)$$

$$CH_3SH + 2OH \rightarrow CH_3S(OH,OH)H \quad (10)$$

$$CH_3SH + OH \rightarrow CH_3S(OH)H \xrightarrow{OH} CH_3SOH + H_2O \quad (11)$$

$$CH_3SH + OH \rightarrow CH_3S(OH)H \xrightarrow{OH} CH_3S(O)H + H_2O \quad (12)$$

Reaction paths 1 and 2 correspond to H abstractions from the SH and CH_3 groups, respectively, and attractive complexes in the entrance channel of the reaction were found for both channels. Reaction path 3 corresponds to the formation of the addition adduct, previously proposed in literature, where the OH radical is added to the sulfur atom in the thiol. Reactions 4 and 5 represent possible evolutions from the adduct formed in 3, where the breaking of the O−H or the S−H bonds, respectively, has been taken into account. Reaction 6 includes the eventual breakage of the C−S bond in the adduct 3, previously suggested by Lee and Tang.[3] Reactions 7−9 include the possible influence of O_2, which is an abundant molecule in troposphere, on the CH_3SH + OH reaction. In reaction 7, the simultaneous addition of OH and O_2 to the sulfur atom is considered, while reactions 8 and 9 involve abstraction reactions from the adduct 3 where the H to be abstracted by the O_2 molecule is the one directly bonded to the S or to the O atom, respectively. Since previous experimental results indicate that the overall rate coefficient increases when the reaction is carried using higher concentrations of OH, paths 10−12 have been included in this work to model the eventual interaction of methyl thiol with two radicals. Channel 10 corresponds to the simultaneous addition of two OH to the sulfur atom, while channels 11 and 12 involve abstraction reactions from the adduct 3 where the H to be abstracted by the second OH is the one directly bonded to the S or to the O atom, respectively.

TABLE 1: Enthalpies (ΔH) and Gibbs Free Energies (ΔG) of Reaction (in kcal/mol) at CCSD(T)/6-311++G(d,p)// BHandHLYP/6-311++G(2d,2p) Level of Theory

channel	ΔH	ΔG
1	−48.74	−49.22
2	−39.46	−40.18
3	−2.93	4.40
4	44.44	47.49
5	22.81	25.38
6	12.11	11.23
7	−1.43	18.73
8	−21.29	−12.24
9	0.34	9.87
10	−27.60	−6.59
11	−89.28	−79.28
12	−67.65	−57.17

The first criterion that we have chosen to select viable paths of reaction is based on the energy change from reactants to products. The enthalpies and Gibbs free energies of reaction for all the modeled paths are reported in Table 1. The electronic energies of all the involved species are provided as Supporting Information (Table S1). Analyzing the stability of the different products, in terms of Gibbs free energies, related to the sum of [G(CH_3SH) + G(OH)], we found that only six of the 12 modeled paths seem to be viable, and they have been highlighted in bold in the table. These paths correspond to processes that are thermodynamically feasible (i.e., with $\Delta G < 0$). According to our results, when the CH_3SH + OH reaction takes place in absence of O_2, and with no excess of OH, only the channels corresponding to H abstractions are likely to occur, leading to the formation of radicals CH_3S and CH_2SH and water. Only on the basis of ΔG, we expected the main channel to be H abstraction from the SH site.

The possible addition of the OH radical to the sulfur atom (channel 3) leading to the formation of a direct addition product was found to be an exothermic but non-exoergic process. Accordingly, the adduct seems to be a weak bond complex and not a proper addition product. Since this specific process has been previously considered as relevant in thiols + OH reactions, it was also modeled at the CCSD(T)/6-311++G(d,p)//MP2/6-311++G(2d,2p) and CCSD(T)/6-311++G(d,p)//B3LYP/6-311++G(2d,2p) levels of theory to establish if the nonexistence of the hypothetical $CH_3S(OH)H$ structure was an artifact of the BHandHLYP functional or an outcome inherent to the chemistry of the studied systems. These methods confirm the formation of a weakly bonded complex ($\Delta G^{(3)}_{R=CH_3,geom=MP2} = 3.78$ and $\Delta G^{(3)}_{R=CH_3,geom=B3LYP} = 3.51$ kcal/mol), which also agrees with the chemical notion that sulfur atoms are not likely to form compounds in which they would have three bonds. For the sake of thoroughness, channel 3 was also modeled for ethyl and *n*-propyl thiols, and the results were similar to that of the methyl thiol (i.e., the ΔG values of the reactions were found to be

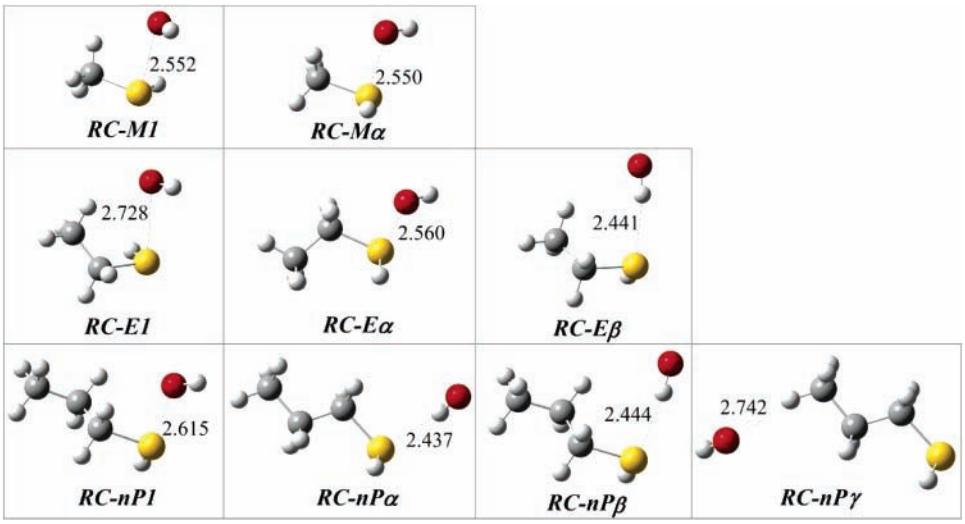

Figure 1. Fully optimized BHandHLYP/6-311++G(2d,2p) abstraction reactant complexes.

positive: $\Delta G^{(3)}_{R=C_2H_5} = 5.00$ and $\Delta G^{(3)}_{R=nC_3H_7} = 4.85$ kcal/mol). These findings suggest that R−S(OH)H species are short-lived, weakly bonded adducts that do not lead to proper addition products and seem to rule out the addition as the main channel for the aliphatic thiol + OH radical reactions. These results agree with the findings of Tyndall and Ravishankara,[8] and according to them the formation of an addition product at the sulfur end is not the explanation for the fact that CH_3SH, C_2H_5SH, and C_3H_7SH react with OH at very similar rates.

In the presence of O_2, which would be the case of the tropospheric reaction, channel 8 also seems to contribute to the overall reaction, leading to the formation of two additional products: CH_3–S−OH and hydrogen peroxide. In contrast to what has been previously reported[25] for the reaction of dimethyl sulfide with OH, in the presence of O_2, channel 7 does not seem to contribute to the overall reaction of methyl thiol. On the other hand, if the reaction takes place in excess OH, the formation of CH_3–S(2OH)−H, CH_3–S−OH, and CH_3–S(O)−H could be expected to some extent, since channels 10−12 were found to be exoergic. Therefore, the increase in OH concentration would lead to a rise in the overall rate of reactions by increasing the number of viable reaction channels. These results are in agreement with the findings of Lee and Tang.[3] According to ΔG values, their relative abundance would be CH_3–S−OH > CH_3–S(O)−H > CH_3–S(2OH)−H. However, since they are not relevant to the tropospheric reaction, they have not been studied in more detail in the present work.

Since reaction 8 was found to be exoergic and this is a path that could be relevant in the troposphere, a search for the corresponding transition state was performed. According to our results, this channel occurs in two steps, namely: (a) the formation of an adduct with the OH bonded to the sulfur atom and the O_2 molecule weakly bonded to the H in the SH site, followed by (b) the H abstraction from the SH site leading to the formation of HO_2. The barrier of the first one was found to be too high to compete with channels 1 and 2 with $\Delta G^{\neq(8a)}_{R=CH_3} = 31.6$ kcal/mol, compared to $\Delta G^{\neq(1)}_{R=CH_3} = 7.1$ and $\Delta G^{\neq(2)}_{R=CH_3} = 9.2$ kcal/mol for channels 1 and 2, respectively. These results agree with the findings of Hynes and Wine[6] that the thiol + reactions are independent of O_2 concentration.

According to the results previously discussed, the only channels relevant to the aliphatic thiol + OH tropospheric reactions seem to be H abstractions from the thiols by the OH radical. The abstraction channels have been modeled using a three-step mechanism: (I) formation of the reactant complex from the isolated reactants, (II) formation of the product complex from the reactant complex, and (III) formation of the corresponding radical and water from the product complex:

$$T + OH \underset{(-I)}{\overset{(I)}{\rightleftharpoons}} RC \xrightarrow{(II)} PC \underset{(-III)}{\overset{(III)}{\rightleftharpoons}} R + H_2O$$

where T represents each thiol, and RC, PC, and R represent the reactant complex, product complex, and radical product corresponding to each particular path.

In all, nine reactant complexes (RC) involved in the modeled H abstraction paths were identified (Figure 1). They were obtained from IRC calculations starting at the corresponding transition state structures. The IRC calculations included 100 points in each direction, and the end points of the IRC corresponding to the reactant side were optimized to minimum to obtain the correct reactant complexes that correspond to each reaction path. All the RCs involved in abstractions from the SH group (RC-M1, RC-E1, and RC-*n*P1) were found to occur through interactions between the O atom in the OH radical and the S atom in the thiols. The same kind of interaction seems to be responsible for the formation of the complexes corresponding to abstractions from α sites in methyl and ethyl thiols (RC-Mα and RC-Eα), while RC-*n*Pα is formed by interaction of the H atom in the OH radical and the S atom in *n*-propyl thiol. The complexes RC-Eβ and RC-*n*Pβ are formed by interactions that are similar to those described for RC-*n*Pα. On the other hand, the reactant complex involved in the H abstraction from the γ site in *n*-C_3H_7–SH was found to be formed through the interaction between the O atom in the OH radical and the H to be abstracted.

Since the distances between the interacting atoms are quite large (Figure 1) and the stabilization energies arising from the complex formations are in most cases about 2 kcal/mol (Table 2), Bader topological analyses[26,27] were performed to confirm that the apparent interactions are not an artifact of the calculations. The Bader analyses calculations were performed using the BHandHLYP/6-311++G(2d,2p) wave functions of the reactant complexes. As is well known, this kind of analysis of the charge density $\rho(r)$ and its Laplacian, $\nabla^2\rho(r)$, identifies critical points that have been imputed to attractive interactions. Two different kinds of critical points were found: bond critical

TABLE 2: CCSD(T)/6-311++G(d,p)//BHandHLYP/6-311++G(2d,2p) Energies (in kcal/mol) Relative to the Isolated Reactants

	CH_3SH		C_2H_5SH		n-C_3H_7S H	
	ΔE^a	ΔG^b	ΔE	ΔG	ΔE	ΔG
RC-1	−2.56	4.40	−1.96	5.00	−2.06	4.85
RC-α	−2.54	4.43	−2.45	4.53	−2.58	3.59
RC-β			−2.89	3.78	−3.03	3.57
RC-γ					−0.73	0.95
TS-1	−0.21	7.08	−0.30	7.32	−0.36	7.29
TS-α	1.69	9.19	−0.20	7.52	−0.74	7.11
TS-β			2.59	10.65	0.13	8.36
TS-γ					3.57	10.77
PC-1	−32.61	−26.73	−31.95	−24.84	−32.25	−27.54
PC-α	−23.36	−18.82	−23.79	−18.65	−21.17	−16.46
PC-β			−18.59	−12.58	−20.95	−14.98
PC-γ					−15.52	−10.26
R-1 + H_2O	−29.73	−30.19	−29.20	−29.76	−29.35	−29.91
R-α + H_2O	−20.70	−21.24	−21.17	−22.19	−20.72	−21.74
R-β + H_2O			−12.53	−13.42	−17.99	−19.24
R-γ + H_2O					−14.60	−15.90

[a] Electronic energies, including ZPE corrections. [b] Free Gibbs energies.

TABLE 3: Electronic Charge Density (ρ) and Its Laplacian, $\nabla^2\rho(r)$, for Bond Critical Points in Weakly Bonded Complexes[a]

		atoms	r	$\nabla^2\rho(r)$
RC-M1	BCP	O, S	0.03368	−0.02450
RC-Mα	BCP	O, S	0.03413	−0.02475
RC-E1	BCP	O, S	0.02368	−0.01850
	BCP	O, H_β	0.00874	−0.00718
	RCP	O, H_{OH}, S, C_α, C_β, H_β	0.00722	−0.00693
RC-Eα	BCP	O, S	0.03332	−0.02443
RC-Eβ	BCP	H_{OH}, S	0.01665	−0.01099
	BCP	O, H_β	0.00666	−0.00548
	RCP	H_{OH}, S, C_α, C_β, H_β, O	0.00515	−0.00527
RC-nP1	BCP	O, S	0.03022	−0.02249
	BCP	O, H_β	0.00832	−0.00705
	RCP	O, S, C_α, C_β, H_β	0.00738	−0.00718
RC-nPα	BCP	H_{OH}, S	0.01820	−0.01041
RC-nPβ	BCP	H_{OH}, S	0.01808	−0.01027
	BCP	O, H_β	0.00418	−0.00367
	RCP	H_{OH}, S, C_α, C_β, H_β, O	0.00409	−0.00374
RC-nPγ	BCP	O, H_γ	0.00494	−0.00411

[a] For atom numbering, see Figure 1.

points (BCP) and ring critical points (RCP). The values of $\rho(r)$ and $\nabla^2\rho(r)$ at these points, for each reactant complex described above, are reported in Table 3. The low values of $\rho(r)$ and $\nabla^2\rho(r)$ indicate that the interactions are weak. However, these values also confirm that the electronic density actually increases in the region between the interacting atoms, and since the corresponding values of the Laplacians are negative the critical points represent covalent interactions. In addition, the values in Table 3 show the expected relationship between interatomic distances and the strength of the interactions, that is, for each kind of interaction, shorter distances correspond to larger absolute values of $\rho(r)$ and $\nabla^2\rho(r)$.

The fully optimized transition state (TS) structures for H abstraction channels are shown in Figure 2, where the distances of the breaking and forming bonds have been explicitly reported. IRC calculations were used to confirm that all of them actually connect the desired reactants and products. It was also confirmed that one imaginary frequency is associated with each of the reported structures. For the abstractions from the SH groups and α sites, the methyl thiol TSs were found to be the latest ones along the reaction coordinate. However, the three O···H and S···H distances are very similar among them. In general, the TSs for the abstractions from the SH sites were found to be earlier than those for α abstractions, which are earlier than those for β abstractions, and the latest one was found to be the TS for the γ abstraction from n-C_3H_7–SH. Even though this is just a qualitative criterion, it indicates that the ease of abstraction should follow the same order. However, since there are other factors that can influence the feasibility of H atom abstractions, the energetics and probably the kinetics of the reactions should be considered before establishing a fair comparison among the different channels.

The product complexes and the radical abstractions products were also fully optimized. However, for the sake of brevity, the discussion of their geometries was not included in this article.

The electronic energies as well as the ZPE correction values for all the studied species are reported as Supporting Information (Tables S1−S3). The relative energies reported in Table 2 show that all the ZPE-corrected energies of the transition states, with the exceptions of those corresponding to abstractions from terminal methyl groups, are lower than those of the isolated reactants. In addition, those corresponding to abstractions from the SH group (channel 1) are very similar: −0.2 kcal/mol for CH_3SH and −0.3 kcal/mol for C_2H_5SH and n-C_3H_7SH. This agrees with the experimental finding that the activation energies of the thiols + OH reactions are negative and with only small differences among them. It is also interesting to notice that the lowest activation free energy of channel 1 corresponds to methyl thiol, which indicates that the partial rate coefficient associated with abstractions from the terminal SH group should be larger for CH_3SH, compared to those for C_2H_5SH and n-C_3H_7SH ($k_{1M} > k_{1E}$, $k_{1M} > k_{1nP}$). As shown in Table 4, this is due to the entropic factor.

Rate Coefficients. The rate coefficients (k) corresponding to all the studied reaction channels that significantly contribute to the overall reaction have been analyzed in terms of conventional TST. Consistent with the reaction mechanism proposed above for the abstraction channels, if k_I and k_{-I} are the forward and reverse rate constants for the first step and k_{II} corresponds to the second step, a steady-state analysis leads to a rate coefficient for each overall reaction channel which can be written as:

$$k = \frac{k_I k_{II}}{k_{-I} + k_{II}} \tag{13}$$

Even though when the energy barrier for k_{-I} is about the same size as that for k_{II}, the entropy change is much larger in the reverse reaction than in the formation of the products. The activation entropy ΔS_{II} is small and negative because the transition state structure is tighter than the reactant complex, while ΔS_{-I} is large and positive because six vibrational degrees of freedom are converted into three translational and three rotational degrees of freedom. On the basis of this assumption, first considered by Singleton and Cvetanovic,[28] and successfully used by Alvarez-Idaboy et al.,[23,24] we can rewrite k as:

$$k = \frac{k_I k_{II}}{k_{-I}} = K_{eq} \cdot k_{II} \tag{14}$$

where K_{eq} is the equilibrium constant between the isolated reactants and the reactant complex, and k_{II} is the rate constant corresponding to the second step of the mechanism (i.e., transformation of the reactant complex into products).

Applying basic statistical thermodynamic principles, we may obtain the equilibrium constant (k_I/k_{-I}) of the fast pre-equilib-

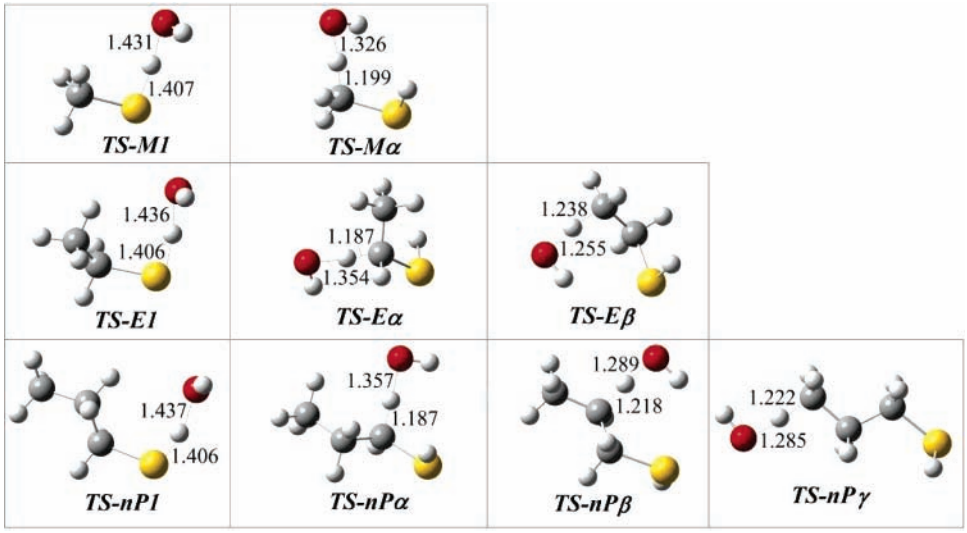

Figure 2. Fully optimized BHandHLYP/6-311++G(2d,2p) abstraction transition states.

TABLE 4: $\Delta H^{\neq}$ and $T\Delta S^{\neq}$ Terms (in kcal/mol) for Hydrogen Abstractions from the SH Site, Related to Isolated Reactants

	$\Delta H^{\neq}$	$T\Delta S^{\neq}$
CH_3SH	−0.88	−7.96
C_2H_5SH	−0.88	−8.20
n-C_3H_7SH	−0.86	−8.15

rium between the reactants and the reactant complex as:

$$K_{eq} = \frac{Q_{RC}}{Q_R} \exp[(E_R - E_{RC})/RT] \qquad (15)$$

where Q_{RC} and Q_R represent the partition functions corresponding to the reactant complex and the isolated reactants, respectively.

In a unimolecular process, under high-pressure conditions, an equilibrium distribution of reactants is established, and the TST formula can be applied[29] to calculate k_{II}:

$$k_{II} = \kappa_{II} \frac{k_B T}{h} \frac{Q_{TS}}{Q_{RC}} \exp[(E_{RC} - E_{TS})/RT] \qquad (16)$$

where κ_{II} is the tunneling factor, k_B and h are the Boltzmann and Planck constants, respectively, and Q_{TS} is the transition state partition function. The energy difference includes the ZPE corrections. The effective rate coefficient of each channel is then obtained as:

$$k = \sigma K_{eq} k_{II} \qquad (17)$$

where σ is the symmetry factor, which accounts for the number of equivalent reaction paths.

We have assumed that the reactant complex undergoes collisional stabilization (i.e., the reaction occurs at the high-pressure limit). We have used this limit as our working hypothesis, since there is no experimental evidence that indicates otherwise. This approach has been previously used to describe OH radical reactions with several VOCs. It is also adequate to account for the experimental negative activation energy observed for the thiols + OH reaction. In a classical treatment, the influence of the complex exactly cancels in eq 17 and the overall rate coefficient depends only on properties of reactants and transition states. However, in the present case, there is a possibility of quantum mechanical tunneling for the abstraction channels, and the existence of the complex means that there are extra energy levels from where tunneling may occur so that the tunneling factor, κ, increases. We have assumed that a thermal equilibrium distribution of energy levels is maintained, which corresponds to the high-pressure limiting behavior. Thus, energy levels from the bottom of the well of the complex up to the barrier might contribute to tunneling.

TABLE 5: Rate Coefficients (in cm^3 $molecule^{-1}$ s^{-1}) and Branching Ratios (Γ) at 298 K

R =	$-CH_3$	$-C_2H_5$	$-nC_3H_7$
$K_{overall}$	1.34×10^{-11}	1.47×10^{-11}	3.03×10^{-11}
Γ^1	0.816	0.228	0.190
G^a	0.184	0.720	0.603
G^b		0.052	0.203
G^g			0.004

It has been assumed that neither mixing nor crossover between different pathways occurs. Thus, the overall rate coefficient (k) for each thiol has been calculated by summing up the partial rate coefficients corresponding to each possible channel.[30] The addition path has not been included since according to the energetic profiles it is very unlikely to contribute to a significant extent to the overall reaction.

Since accurate rate constant calculations require the proper computation of the partition functions (Q), the hindered rotor approximation has been used to correct the Q values corresponding to internal rotations with torsional barriers comparable to RT. Direct inspection of the low-frequency modes of the studied stationary points indicates that there are several modes that correspond to hindered rotations. These modes should be treated as hindered rotors instead as vibrations.[31] To make this correction, these modes were removed from the vibrational partition function of the corresponding species and replaced with the hindered rotor partition function (Q^{HR}). In our calculations, we have adopted the analytical approximation to Q^{HR} for a one-dimensional hindered internal rotation proposed by Ayala and Schlegel.[32]

The values of the overall rate coefficients at the studied temperatures are reported in Table 5, together with the branching ratios (Γ) corresponding to the different abstraction channels. They have been calculated as:

$$\Gamma^{1,\alpha,\beta \text{ or } \gamma} = \frac{k^{1,\alpha,\beta \text{ or } \gamma}}{k^{overall}} \qquad (18)$$

TABLE 6: Kinetic Isotopic Effects for the Overall Reactions and Tunneling Factors (κ) for Each Reaction Channel (Compared to Those of Nondeuterated Species) at 298 K

	KIE	k
CH_3SD	2.71	1.80 (2.44)
CD_3SH	1.21	3.07 (7.26)
CH_3CH_2SD	1.20	1.77 (2.02)
CH_3CD_2SH	2.78	2.32 (2.96)
CD_3CH_2SH	1.05	7.76 (22.38)
$CH_3CH_2CH_2SD$	1.17	1.68 (2.03)
$CH_3CH_2CD_2SH$	2.12	2.22 (2.59)
$CH_3CD_2CH_2SH$	1.23	4.18 (6.78)
$CD_3CH_2CH_2SH$	1.00	4.85 (10.44)

The calculated rate coefficients agree very well with the previously reported experimental values, differing less than 1 order of magnitude and following the same tendency. As can be seen from the values in Table 5, the abstraction from the −SH site is the main channel of reaction for the CH_3SH + OH system. However, as the size of the thiol increases, its contribution to the overall reaction decreases. The good agreement between the calculated branching ratio $\Gamma_{R=CH_3}$[1] and those reported by Butkovskaya and Setser[9] and Hynes and Wine[6] seems to support the other branching ratios reported here. The significant contribution of the abstraction from the functional group to the overall reaction is quite larger in thiols than it is in alcohols: 84, 26, and 21% compared to 36, 15, and 5%.[33] These larger contributions seem to explain the fact that the rate coefficients of aliphatic thiols + OH are higher than those of aliphatic alcohols. They also seem to explain the fact that the ratios $k_{R=C_2H_5}/k_{R=CH_3}$ and $k_{R=C_3H_7}/k_{R=CH_3}$ for thiols are significantly smaller than the equivalent ratios for alcohols. In addition, the rate coefficients for the abstractions from the −SH sites, which can be easily obtained by multiplying the overall rate coefficient by Γ[1], show the tendency expected from the $\Delta G^{\neq}$ values, that is, $k^{(1)}_{R=CH_3} > k^{(1)}_{R=C_2H_5}$ and $k^{(1)}_{R=CH_3} > k^{(1)}_{R=nC_3H_7}$.

Kinetic Isotopic Effects (KIE). The kinetic isotopic effects were also calculated for all the studied abstraction channels, since they are known to be relevant in proton-transfer reactions, where the occurrence of significant tunneling is highly probable. The KIEs were calculated as

$$\mathrm{KIE} = \frac{k_H}{k_D} \tag{19}$$

where k_H represents the overall rate coefficient of the reaction involving nondeuterated thiols, while k_D represents the overall rate coefficient corresponding to deuterated species.

Different substitution of hydrogen atoms by deuterium were modeled according to the possible abstraction sites. The KIE values, corresponding to overall reactions, as well as the tunneling factors for each channel are reported in Table 6.

As the values in the table show, the largest KIE for methyl thiol + OH reaction occurs when the isotopic substitution involves the sulfur end. For this thiol, Hynes and Wine[6] found the reaction of CD_3SH to be 13% slower than that of CH_3SH. Our calculation for the same reaction is in very good agreement with their experimental determination (17% slower). However, whereas in 1984 Wine et al.[4] found the rate coefficients of the CH_3SD and CH_3SH reactions almost identical, our calculations predict the CH_3SD reaction to be about 60% slower than that of CH_3SH. Further research in this direction would be of great help to solve this discrepancy.

There are no previously reported data on the possible kinetic isotopic effects involving thiols other than CH_3SH. Our calculations predict that the largest KIE values for C_2H_5SH and C_3H_7-SH are expected to be found when isotopic substitutions take place in the α sites. The values are practically negligible when the methyl ends are deuterated. This is mainly due to the very small contribution that abstractions from terminal methyls make to the overall reactions. On the other hand, the expected decreasing in tunneling effect was found for all the deuterated species.

Conclusions

Twelve possible channels have been modeled for the OH + aliphatic thiols reactions, three of them including the possible influence of molecular oxygen, and three of them involving excess OH. The presence of O_2 does not seem to have a significant effect on the reaction, while the excess of OH seems to increase the overall reaction rate by increasing the number of viable paths. According to our results, the only channels that significantly contribute to the overall reaction (for systems with no O_2 and no OH excess) are the hydrogen abstractions from the −SH group and from the alkyl groups. Our results also show that abstractions from the functional group contribute to the overall reaction of thiols to a larger extent than they do in alcohols. In addition, our results indicate that the partial rate coefficient corresponding to abstraction from the −SH group in CH_3SH is larger than those of C_2H_5SH and nC_3H_7SH, which were found to be caused by entropic factors. This peculiarity of the reaction between OH and aliphatic thiols makes the rate corresponding to the smallest member of the family relatively large and consequently closer to those of the larger thiols. The results proposed in the present work seem to provide a viable explanation for the diverse findings previously reported from experimental investigations.

Acknowledgment. We gratefully acknowledge the financial support from the Instituto Mexicano del Petróleo (IMP) and thank the IMP Computing Center for supercomputer time on SGI Origin 3000.

Supporting Information Available: Electronic energies and ZPE correction values corresponding to all modeled nondeuterated species. This material is available free of charge via the Internet at http://pubs.acs.org.

References and Notes

(1) Urbanski, S. P.; Wine, P. H. In *S-Centered Radicals*; Alfassi, Z. B., Ed.; Wiley: Chichester, 1999; pp 97−140.
(2) Bremner, J. M.; Steele, C. G. *Adv. Microb. Ecol*. **1978**, *2*, 155.
(3) Lee, J. H.; Tang, I. N. *J. Chem. Phys*. **1983**, *78*, 6646.
(4) Wine, P. H.; Thompson, R. J.; Semmes, D. H. *Int. J. Chem. Kinet*. **1984**, *16*, 1623.
(5) Barnes, I.; Bastian, V.; Becker, K. H.; Fink, E. H.; Nelsen, W. *J. Atmos. Chem*. **1986**, *4*, 445.
(6) Hynes, A. J.; Wine, P. H. *J. Phys. Chem*. **1987**, *91*, 3672.
(7) Hatakeyama, S.; Akimoto, H. *J. Phys. Chem*. **1983**, *87*, 2387.
(8) Tyndall, G. S.; Ravishankara, A. R. *J. Phys. Chem*. **1989**, *93*, 4707.
(9) Butkovskaya, N. I.; Setser, D. W. *J. Phys. Chem. A* **1999**, *103*, 6921.
(10) Frisch, M. J.; Trucks, G. W.; Schlegel, H. B.; Scuseria, G. E.; Robb, M. A.; Cheeseman, J. R.; Zakrzewski, V. G.; Montgomery, J. A., Jr.; Stratmann, R. E.; Burant, J. C.; Dapprich, S.; Millam, J. M.; Daniels, A. D.; Kudin, K. N.; Strain, M. C.; Farkas, O.; Tomasi, J.; Barone, V.; Cossi, M.; Cammi, R.; Mennucci, B.; Pomelli, C.; Adamo, C.; Clifford, S.; Ochterski, J.; Petersson, G. A.; Ayala, P. Y.; Cui, Q.; Morokuma, K.; Malick, D. K.; Rabuck, A. D.; Raghavachari, K.; Foresman, J. B.; Cioslowski, J.; Ortiz, J. V.; Stefanov, B. B.; Liu, G.; Liashenko, A.; Piskorz, P.; Komaromi, I.; Gomperts, R.; Martin, R. L.; Fox, D. J.; Keith, T.; Al-Laham, M. A.; Peng, C. Y.; Nanayakkara, A.; Gonzalez, C.; Challacombe, M.; Gill, P. M. W.; Johnson, B.; Chen, W.; Wong, M. W.; Andres, J. L.; Gonzalez, C.; Head-Gordon, M.; Replogle, E. S.; Pople, J. A. *Gaussian 98*, revision A.3; Gaussian, Inc.: Pittsburgh, PA, 1998.
(11) Eyring, H. *J. Chem. Phys*. **1935**, *3*, 107.

(12) Truhlar, D. G.; Hase, W. L.; Hynes, J. T. *J. Phys. Chem.* **1983**, *87*, 2664.
(13) Eckart, C. *Phys. Rev.* **1930**, *35*, 1303.
(14) Truong, T. N.; Truhlar, D. G. *J. Chem. Phys.* **1990**, *93*, 1761.
(15) Truong, T. N. *J. Phys. Chem. B* **1997**, *101*, 2750.
(16) Truong, T. N.; Duncan, W. T.; Tirtowidjojo, M. *Phys. Chem. Chem. Phys.* **1999**, *1*, 1061.
(17) Truhlar, D. G.; Isaacson, A. D.; Skodje, R. T.; Garrett, B. C. *J. Phys. Chem.* **1982**, *86*, 2252.
(18) Mora-Diez, N.; Alvarez-Idaboy, J. R.; Boyd, R. J. *J. Phys. Chem. A* **2001**, *105*, 9034.
(19) Alvarez-Idaboy, J. R.; Galano, A.; Bravo-Pérez, G.; Ruiz-Santoyo, Ma. E. *J. Am. Chem. Soc.* **2001**, *123*, 8387.
(20) Galano, A.; Alvarez-Idaboy, J. R.; Bravo-Perez, G.; Ruiz-Santoyo, Ma. E. *Phys. Chem. Chem. Phys.* **2002**, *4*, 4648.
(21) Galano, A.; Cruz-Torres, A.; Alvarez-Idaboy, J. R. *J. Phys. Chem. A* **2006**, *110*, 1917.
(22) Alvarez-Idaboy, J. R.; Cruz-Torres, A.; Galano, A.; Ruiz-Santoyo, Ma. E. *J. Phys. Chem. A* **2004**, *108*, 2740.
(23) Alvarez-Idaboy, J. R.; Mora-Diez, N.; Boyd, R. J.; Vivier-Bunge, A. *J. Am. Chem. Soc.* **2001**, *123*, 2018.
(24) Alvarez-Idaboy, J. R.; Mora-Diez, N.; Vivier-Bunge, A. *J. Am. Chem. Soc.* **2000**, *122*, 3715.
(25) Gross, A.; Barnes, I.; Sørensen, R. M.; Kongsted, J.; Mikkelsen, K. V. *J. Phys. Chem. A* **2004**, *108*, 8659.
(26) Bader, R. F. W. *Atoms in Molecules: A Quantum Theory*; Oxford University Press: Oxford, 1990.
(27) Bader, R. F. W.; MacDougall, P. J.; Lau, C. D. *J. Am. Chem. Soc.* **1984**, *106*, 1594.
(28) Singleton, D. L.; Cvetanovic, R. J. *J. Am. Chem. Soc.* **1976**, *98*, 6812.
(29) Pilling, M. J.; Seakins, P. W. *Reaction Kinetics*; Oxford University Press: New York, 1996.
(30) Robinson, P. J.; Holbrook, K. A. *Unimolecular Reactions*; Wiley-Interscience: London, 1972.
(31) Jacox, M. E. *Vibrational and Electronic Energy Levels of Polyatomic Transient Molecules*; American Chemical Society: Washington, DC and American Institute of Physics: New York, 1998; Vol. 69, p 945.
(32) Ayala, P. Y.; Schlegel, H. B. *J. Chem. Phys.* **1998**, *108*, 2314.
(33) Galano, A.; Alvarez-Idaboy, J. R.; Bravo-Perez, G.; Ruiz-Santoyo, Ma. E. *Phys. Chem. Chem. Phys.* **2002**, *4*, 4648.